Toward Vision-based Adaptive Configuring of A Bidirectional Two-Segment Soft Continuum Manipulator

Jiewen Lai, Kaicheng Huang, Bo Lu and Henry K. Chu*

Abstract—In soft robotics, developing an effective way of robot-environment interaction is a challenging task due to the soft nature of the material that makes the manipulator. This paper demonstrates a vision-based approach to configure a two-segment soft continuum robot manipulator into an user-defined configuration and interact with unknown objects on plane. The soft robot manipulator actuated by cable-driven mechanism, is composed of two cascade continuum segments which are made from poly-dimethyl-siloxane (PDMS). The overall robot configuration can be determined in a point-wise manner on image plane provided by an eye-to-hand system. One can define the end-effectors' location on the visual system to re-shape the manipulator. The visual servoing fashion allows the robot to optimize its gesture to its best fit without developing any complicated model. Experiments on prototype indicate that the proposed model-free approach can be well employed, even when the manipulator is bearing a payload. By adaptively adjusting the manipulator's stiffness to a quasi-deadlock status, the payload capacity is up to nearly 6 times of the manipulator's mass itself.

I. INTRODUCTION

Continuum robots are of interest to roboticists in recent decades since its very early appearance [1] [2]. Theoretically, a continuum robot is characterized as a dexterous robot manipulator with infinite degrees of freedom (DOFs). The inherent dexterity empowers the continuum robots to work in sinuous and multi-constrained surroundings that conventional robot arms are struggling to set foot in. In recent years, a trend of developing continuum robot body using soft material is in vogue. The softness gifts high deformability and energy-absorbing properties to the continuum robot [3]. A great number of foreseeable applications can be innovated by utilizing the soft continuum robots, whereas minimally invasive surgery (MIS) is one of the most promising fields [4]. In MIS, the robot manipulator is designed to go through millimeter-grade incision(s) to provide online diagnosis and in situ treatment via its dexterous manipulator [5]. Before the continuum robot can be employed in MIS, it has to meet several prerequisition which are essential for human-robot interaction safety, such as the precise manipulation in the fragile intra-cavity (or organs) environment and interactive adaption to the external disturbance. The compliant nature of soft continuum robot provides an option to tackle those challenges.

J. Lai, K. Huang, and H. K. Chu are with the Department of Mechanical Engineering, The Hong Kong Polytechnic University, Hung Hom, KLN, Hong Kong.{jw.lai, kaicheng.huang} @connect.polyu.hk

B. Lu is with the T Stone Robotics Institute, The Chinese University of Hong Kong, Shatin, NT, Hong Kong. bolu@cuhk.edu.hk

*Corresponding author: *Henry K. Chu*. henry.chu@polyu.edu.hk

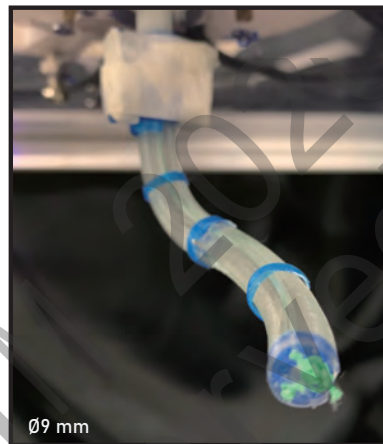A supplementary video can be found here: https://youtu.be/_yy3LjOx5cc

Fig. 1. Prototype of a two-segment soft continuum manipulator.

The precision control of a soft robot requires a reliable approach of perceiving its real-time state. However, it comes at the cost of developing complicated mathematical exact model in terms of controlling the robot tip/shape [6], and it can be even more difficult when it is in the presence of unknown disturbances. With prior knowledge to the dynamic model of the robot, a soft manipulator can interact with environment based on the haptic feedback from its sensors. Thus far, various on-board sensors have been utilized [7], including an optical fiber Bragg grating (FBG) which is capable of shape reconstruction and haptic sensing [8] [9]. A resistive transducer which makes use of metal liquid called eutectic gallium–indium (eGaIn) has been embedded into the silicone to realize deformation perception and force detection [10]. Case *et al.* demonstrate a model for multi-segment proprioceptive continuum robot that wrapped with pneumatic jacket [11]. The aforementioned robot-sensor integration endows the soft robot with proprioception in a costly way because of the built-in sensing, and the complicated fabrication makes the robot with on-board sensing rather delicate. None of these demonstrate corrections for external loads.

Alternatively, vision-based sensing can be an inexpensive approach for the perception of soft robot system. Wang *et al.* develop an eye-in-hand platform to servo the soft manipulator in constrained environment with an adaptive controller [12]. Fang *et al.* propose a machine-learning approach to control an eye-in-hand soft robot [13]. The motion mapping matrices can be updated online when an external load is added to the robot and the robot can still maintain the desired shape. Similarly, Kudryavtsev *et al.* design a visual

servoing controller for an eye-in-hand concentric tube robot [14]. However, the operating principle is different from soft robots as the bending angle is one of the control parameters. Wang *et al.* propose an eye-to-hand method, in which the camera is mounted at the manipulator base internally [15]. A pre-trained convolutional neural network is implemented to reconstruct the manipulator shape which is based on the pre-patterned color inside the hollow structure. Bruder *et al.* propose a predictive approach for positioning a soft robot to follow a path [16]. While finding the control inputs is an non-convex optimization problem, in their work, the path is first transformed to the lifted space and visual data are used to model predictive controller design. While soft robots today with higher power outputs are able to perform more sophisticated tasks, little work has yet been done on compensating soft robot subjected to external loads.

As for as soft-bodied manipulator, it should be acknowledged that the elongation and deformation of the robot material which is not necessarily to be linear are to be pre-parameterized in the perfection of modeling, and it can be more complicated in the presence of interactive environment. It motivates people to adhere endless on-board sensors onto the robot resulting a massive computation. It is a challenging task to build an analytical representation while the highly-deformable manipulator is encounter with obstacle or external forces. Even if within the same shape, the stiffness of the soft manipulator can be a variate subjected to different tasks.

In this paper, we develop a vision-based method to servo a two-segment soft continuum manipulator to a specific gesture as much as possible in a planar domain without on-board sensing. We are interested in shaping a two-segment soft robot into a user-defined posture regardless of the external payload. The soft-bodied robot is mainly made from elastomer and 3D-printed material. The soft robot we developed follows a classic cable-driven mechanism [12] [17], in which manipulator can be actuated via changing the actuation length of cables (Fig. 1). Two segments are assembly in series. Colored labels are attached along the manipulator isometrically as features for visual detection. The robot status will be updated using an image-based sensing technique. Instantaneous measurement attained from the visual feedback is treated as the new input to the robot control loop. On top of that, the soft robot can also passively adjust its stiffness to reach the assigned posture even when it is bearing a payload nearly six times of the manipulator's mass. The proposed approach is competent of posing the two-segment soft robot into different shapes with environment interaction. The approach may help to explore the work-ability of miniaturized soft-bodied robot in complex environment.

The rest of this paper is structured as follows. Section II introduces the visual servoing method and the control scheme for a 2-segment manipulator. Section III demonstrates the prototyping of the soft robot and the experimental setup. Experiment results are shown in Section IV. And Section V summarizes the work.

II. METHOD

In this paper, we implement the image-based visual servoing (IBVS) to control a two-segment soft robot manipulator. Since we only use a stationary monocular vision, the robot is manipulated in 2D although the prototype is capable of 3D (6-DOF) motion. The camera which is fixed with respect to the global reference frame observes the manipulator's motion. Error is computed directly on the values of the robot features extracted from the image plane without reconstructing its configuration. The robot shall move accordingly so as to minimize the error between the current values and the desire values until it reaches the threshold, i.e., to regulate the the error vector $e = \mathbf{s} - \mathbf{s}^*$ to minimum, where $\mathbf{s}$ is the visual feature coordinate, and $\mathbf{s}^*$ is the goal feature [18].

A. Visual Servoing Control of Two-Segment Soft Robot

The end-effector position $\mathbf{x} \in \mathbb{R}^n$ of a cable-driven soft manipulator can be controlled by giving a set of cable actuation as inputs $\mathbf{q} \in \mathbb{R}^m$, such that

$$\mathbf{x} = f(\mathbf{q}). \tag{1}$$

The manipulator velocity can be attained by taking the time derivative of Eq. (1) as

$$\dot{\mathbf{x}} \approx \mathbf{J}\dot{\mathbf{q}} \tag{2}$$

where $\mathbf{J} \in \mathbb{R}^{m \times n}$ is the Jacobian matrix that linearly estimate the instantaneous change of end-effector in response to the actuation. The Jacobian matrix is described as

$$\mathbf{J} = \begin{bmatrix} \dfrac{\partial \mathbf{x}^\top}{\partial \mathbf{q}_1} & ... & \dfrac{\partial \mathbf{x}^\top}{\partial \mathbf{q}_m} \end{bmatrix}. \tag{3}$$

A model-free visual servoing controller requires an initial estimation of the Jacobian matrix ($\mathbf{J}_0$), which can be obtained by incrementally actuating each input and measuring the position displacement of the end-effector in image plane accordingly. As the manipulator moves, the Jacobian will be constantly updated based on the visual feedback regardless of its environment. At time step t, the incremental input $\Delta \mathbf{q}_t$ is yielded by

$$\Delta \mathbf{q}_t = \mathbf{J}_t^\dagger \Delta \mathbf{x}_d \tag{4}$$

where $\mathbf{J}_t^\dagger$ is the Moore–Penrose pseudo-inverse of Jacobian matrix at time step t as $\left(\mathbf{J}_t^\top \mathbf{J}_t\right)^{-1} \mathbf{J}_t^\top$, and $\Delta \mathbf{x}_d$ denotes the desired end-effector move at time step t given by the reference position and current position, i.e., $\Delta \mathbf{x}_d = (\mathbf{x}_r - \mathbf{x}_t)$. In image plane, we consider the manipulator motion plane is parallel to the camera plane, such that, $\mathbf{s}_t = \mathbf{s}_{\mathbf{x}_t}$. The end-effector position at time step t is $\mathbf{x}_t = [u_t, v_t]^\top$. The reference position of end-effector is $\mathbf{x}_r = [u_r, v_r]^\top$, which is related to the current position $\mathbf{x}_t$ and goal position $\mathbf{x}_g = [u_g, v_g]^\top$ as

$$\begin{bmatrix} u_r \\ v_r \end{bmatrix} = \begin{bmatrix} u_t \\ v_t \end{bmatrix} + \frac{\alpha}{\|\mathbf{x}_g - \mathbf{x}_t\|} \begin{bmatrix} u_g - u_t \\ v_g - v_t \end{bmatrix} \tag{5}$$

where α is the damping unit. The online continuous estimation of Jacobian at time step $\mathbf{J}_{t+1}$ can be formulated as

$$\begin{aligned}
\underset{\mathbf{J}_{t+1}}{\text{minimize}} \quad & \|\Delta\mathbf{J}_t\|_F \\
\text{subject to} \quad & \Delta\mathbf{x}_t = \mathbf{J}_{t+1}\Delta\mathbf{q}_t \\
& \mathbf{J}_{t+1} = \mathbf{J}_t + \eta\Delta\mathbf{J}_t
\end{aligned} \qquad (6)$$

where $\|\cdot\|_F$ is the Frobenius norm to be minimized, and $\eta \in [0,1]$ is the buffer constant for Jacobian update.

Summarizing (4)-(6), a position-based proportional tracking control law can be designed as

$$\mathbf{q}_{t+1} \leftarrow \mathbf{q}_t + \lambda\left(\mathbf{J}_{t+1}^\dagger \Delta\mathbf{x}_d\right) \qquad (7)$$

where λ is the proportional gain to ensure a smooth motion. For one single soft segment, the controller frameworks is shown in Fig. 2.
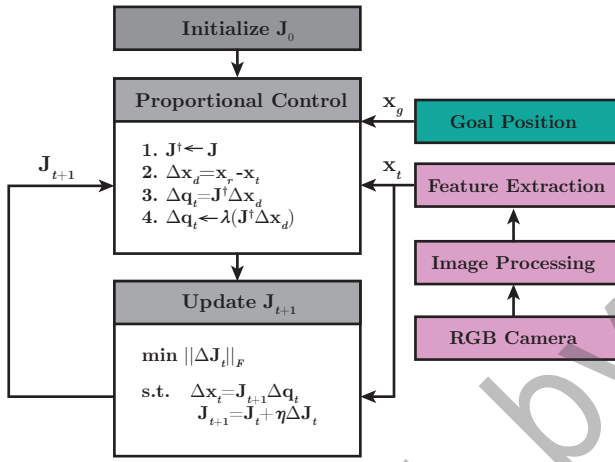
Fig. 2.   Controller architecture of a single soft segment.

Two-segment soft continuum manipulator is articulating two soft modules, while the cables of the distal segment are coupled in the distal one. Ideally, regardless of the cable-channel friction, if the soft module is stiff enough when being actuated, each segment can be independently controlled without considering coupling. In fact, by defining goal positions for each module (i.e, the proximal goal point $\mathbf{x}_{g1}$ and the distal goal point $\mathbf{x}_{g2}$), it is not necessary for the robot to deadlock its segmental gesture to reach the goal points. Therefore, the motion of the distal segment will deviate the previous segment (Fig. 3).

In order to control both end-effectors to reach their desired goal position, an iterative method can be used. A soft module can become stiffer by proportionally actuating all their cables. As shown in Fig. 4, the visual feedback constantly tracks the module end-effectors. Each segment is controlled as schemed in Fig. 2, until the norm of current position and goal position reach the threshold of ε pixels. It shall be noted that the definition of $\mathbf{x}_{g1}$ happens before that of $\mathbf{x}_{g2}$ to ensure a unique solution.

Following aforementioned approach, the soft manipulator is capable of adapting the unknown payload by adjusting the modular stiffness in due course. Experiment will be shown in the next section.
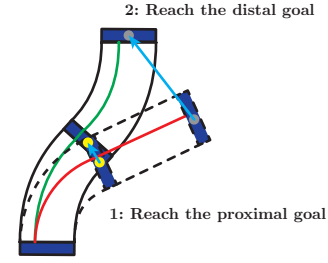
Fig. 3.   The actuation of distal end-effector (gray) will deviate the proximal end-effector (yellow) from its reached position, since and cables of the distal are couple in the proximal one, and the proximal module is soft.
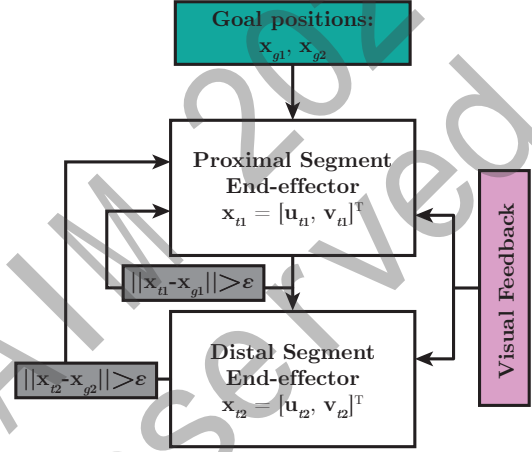
Fig. 4.   Control scheme for 2-segment soft manipulator.

III. PROTOTYPE AND EXPERIMENT

A. Prototype Design and Experimental Setup

The soft continuum manipulator in this paper is composed of two independent segments. The distal segment has 3 concentrically distributed channels, while the proximal segment has 6. Each soft segment is 50 mm in length, with a diameter of 9 mm. The fabrication process is outlined as in Fig. 5. For the proximal segment, 6 straight Nitinol rods are assembled into the respective holes of a 3D printed end disk (Ø8.5mm) which is made from blue polylactic acid (PLA). A 3D printed mold (PLA) is employed to cast the cylindrical shape segment. Poly-dimethyl-siloxane (PDMS) base and its curing agent (SYLGARD 184, Dow Corning, MI, USA) are pre-mixed with a mass ratio of 10:1 according to the product description. After the degassing procedure, the liquid mixture is injected into the mold. The filled mold goes through a 85°C water-bath process to cure for 2 hours before it can be disassembled. Dyneema wires (Royal DSM, Netherlands) with a diameter of 0.4 mm are then run through the corresponding channel, and knots are tied at the end disk side. The distal segment is made following the similar method, but with longer wires which are going through the unassigned channels in the proximal segment. The total mass of the two soft segments is approx. 8 g.

The experiment platform setup is shown in Fig. 6. In the experiment, monocular vision is employed for the planar manipulator motion tracking. A USB camera (Microsoft®
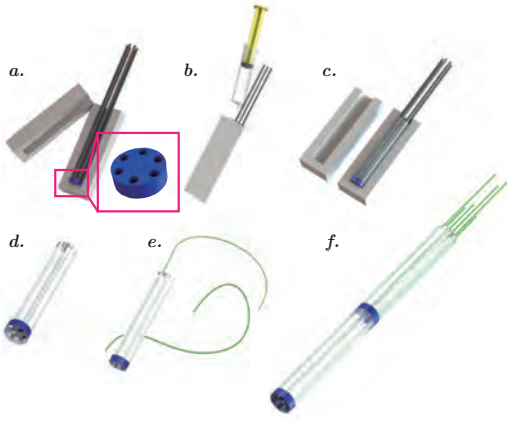
Fig. 5. The manufacturing procedure of a two-segment soft continuum manipulator prototype. (a) components assembly (b) pre-mixed and degassed PDMS mixture injection (c) disassembly (d) single soft continuum body (e) Dyneema wires guiding (f) prototype of final assembly.
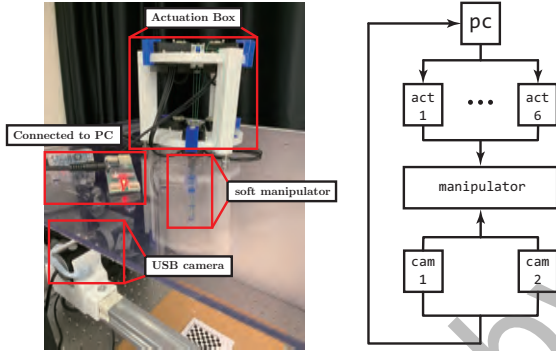

Fig. 6. Left: Experiment setup. The servo motors are installed on a two-story 3D printed box in a circular pattern with an angle of 120° to each other. Right: System diagram.

LifeCam Cinema, WA, USA) is used, and the streaming format is 640×480 pixel in 30 fps. The experiment platform is controlled via a 64-bit PC with an 2.20GHz Intel Core i7-8750H CPU and 16GB RAM. The features of the manipulator are the proximal and distal end-effector, which are distinguished by blue PLA. The middle point of each segment is also wrapped by a thin layer of blue PLA ring as marker to visualize the moves in image. The cables are tied to Dynamixel XM430 servo motors (ROBOTIS Co.,Ltd., Seoul, Korea), which are controlled by using the product bulit-in library functions on MATLAB.

B. Visual Tracking of Features

The visual tracking system is implemented in MATLAB with Image Acquisition Toolbox and Image Processing Toolbox. The vision background is set as a white board. While streaming, each frame is captured as an RGB image. As shown in Fig. 7, the RGB image is transformed into gray image and binarized before the blue elements are subtracted. To improve the detection accuracy, basic morphological operations are conducted for each frame, such as pixel dilation and erosion. We find out the contour centroids of the outstanding pixels (white clusters in Fig. 7(c)) which outlines the manipulator shape. Centroids are sorted once five objects are detected simultaneously. To stabilize the tracking in real-time video stream, Kanade–Lucas–Tomasi (KLT) tracker is used to link the registered features in successive frames, so that a steady tracking can be ensured.

C. Experiment

The goal positions, which are the end-effector position of proximal ($\mathbf{x}_{g1}$) and distal ($\mathbf{x}_{g2}$) segment, are manually defined by mouse-click at the beginning of streaming once the manipulator is recognized. The aim of this experiment is that we want the manipulator to be reshaped as much as possible by only two user-defined goal positions. Therefore, the set goal positions shall be reasonable. To this end, assuming the soft manipulator is rigid, its end-effectors' workspace can be roughly considered as a circle whose origin is the segmental base and the radius as segment length at its rest state. Such that, the frame-based assisted circles for both segments will be plotted out on the RGB image (Fig. 8) to guide the user setting at the beginning. The manipulator status is constantly updated on the image and is also used as a visual feedback to the controller. The damping unit is set as $\alpha = 0.1$, the buffer constant for Jacobain update is $\eta = 0.5$, and the proportional gain $\lambda = 0.5$ (mentioned in Section II).

However, the proposed assisted circles are only to guide the user to reasonably define the location of the distal tip points. It should be acknowledged that the assisted circle is not initiated as the constant curvature assumption of the soft manipulator. The feasibility and accuracy of reaching the user-defined position depends on how far the desired point deviate from the assisted circle. The accuracy of the tips approaching the user-defined points is satisfactory within 90 degrees bending for each segment.

IV. RESULT AND DISCUSSION

In this experiment, the pixel threshold is set as $\varepsilon = 20$ pixels, since the user-defined goals are not exactly reachable in the first place. The total length of the soft manipulator at rest state in image plane is about 310 pixel, which makes the final error within 6.5%.

A. Shaping Without Payload

The benefit of a two-segment soft manipulator is that it can be shaped as an "S" gesture that a single segment manipulator cannot achieve. In this subsection, several manipulator gesture are tested using the aforementioned model-free visual servoing method, including the "S" shape, the "C" shape, and the "J" shape. The intuitive results are shown in Fig. 9. The result indicates the fact that the actuation of each soft module affects to the other. The proposed control scheme in this paper is able to adaptively adjust the stiffness of finished segment in order to control the other, i.e., to maintain the proximal end-effector to its goal position as much as possible (within ε) and manipulator the distal tip at the same time. From Fig. 9, we can notice that the left side gestures (Fig. 9(a,c)) perform better than those on the right (Fig. 9(b,d)).

Fig. 7. Manipulator recognition via feature detection. The manipulator is labeled with three blue markers, while the proximal and distal end-effector (disk) are embedded inside the PDMS body. The image resolution is 640×480 pixel. (a) RGB image; (b) gray scale image with blue elements are subtracted; (c) binarized image; (d) centroid assignment based on contour recognition; (e) labeled RGB image.
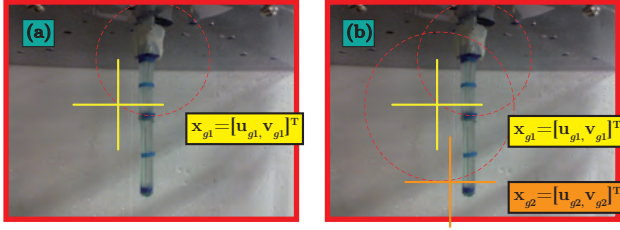

Fig. 8. The end-effector goal positions are mouse-clicked in the image frame once the manipulator is recognized. Selected goals shall be roughly near the respective circular line. (a) Defining $\mathbf{x}_{g1} = [\mathbf{u}_{g1}, \mathbf{v}_{g1}]^\top$; (b) defining $\mathbf{x}_{g2} = [\mathbf{u}_{g2}, \mathbf{v}_{g2}]^\top$ based on the $\mathbf{x}_{g1}$.

The chattering in Fig. 9(b,d) is because the manipulator is designed with 3 cables per segment which allows the robot to manipulate in 3D, and moving to the opposite planar side (which is right-hand side in this case) requires the other two cables to be actuated simultaneously. Therefore, the doubled force generates an overshoot and triggers an iterative correction process which performs like chattering. And also, the reference of final steady state error is the user-defined points, which are not necessarily a reachable location. Without specifying a stiffness, the manipulator is set to be paused when the feature points start to deviate twice from the current best.

By setting the damping and proportional gain to the controller, the proposed method realizes a steady convergence in terms of tip error. In most cases, the end-effectors can reach their steady-state error within several dozens of iteration. The iteration time depends on the processing speed.

B. Shaping with Payload

The merit of implementing visual servoing control in a cable-driven soft robot is that, the robot can adapts its stiffness to the external forces. Constrained by the soft nature, a soft manipulator shall not able to bend with a payload out-weights its capacity within the same stiffness. However, stiffening this soft beam-like structure helps to enhance the rigidity of the manipulator. In cable-driven soft robot, the stiffness of the manipulator can be changed by applying certain amount of force to the cables. The modeling of actuation and stiffness is rather complicated because of the non-linearity of the elastomer properties. A model-free approach allows the manipulator stiffness to be compensated according to the error which awaited to be minimized. To this extent, several loading tests are done to evaluate the manipulator's capacity of bearing weight. The net weight of the two-segment continuum soft manipulator (including PDMS body, 3D-printed blue rings as embedded disks, blue markers, cables) is 8.2g. Results are shown in Fig. 10.

In Fig. 10(a), the manipulator's tip is crammed into a 9-mil bullet casing (inner diameter is 9.03 mm). The task is to move the object (weight is unknown to the robot) to the specified goal position $\mathbf{x}_{g2}$ (black dot at the image) rightward to the manipulator, while keeping the proximal segment still. The goal position for the proximal segment $\mathbf{x}_{g1}$ is set near
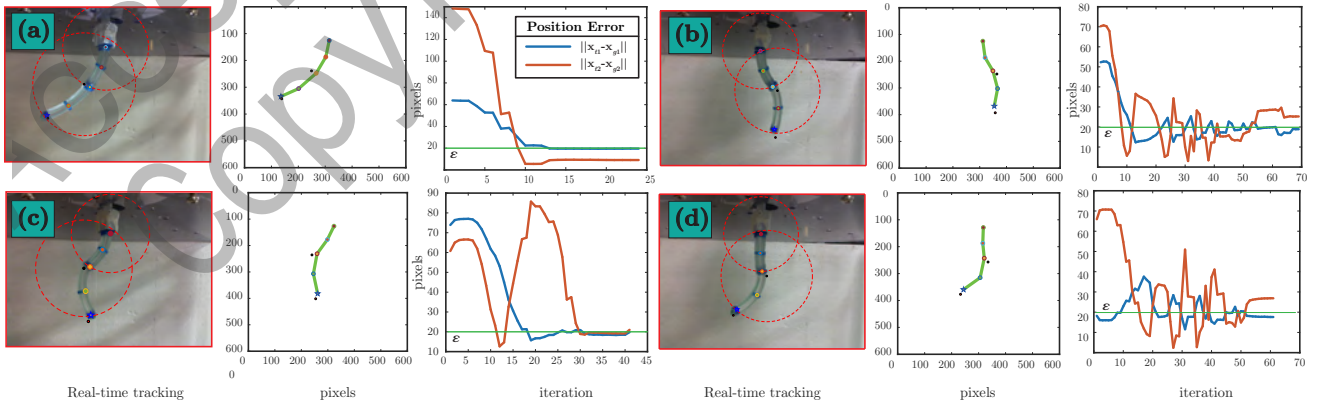

Fig. 9. Configuring the a two-segment soft manipulator into different gestures. The RGB images show the finalized manipulator status in the real-time tracking. The second and fifth row give a clearer re-constructed view of the manipulator in pixel axis. The error plots return the iteratively updated positional error of both end-effectors. The threshold ε is 20 pixels. (a) inverted C-shape; (b) S-shape; (c) inverted S-shape; (d) J-shape;
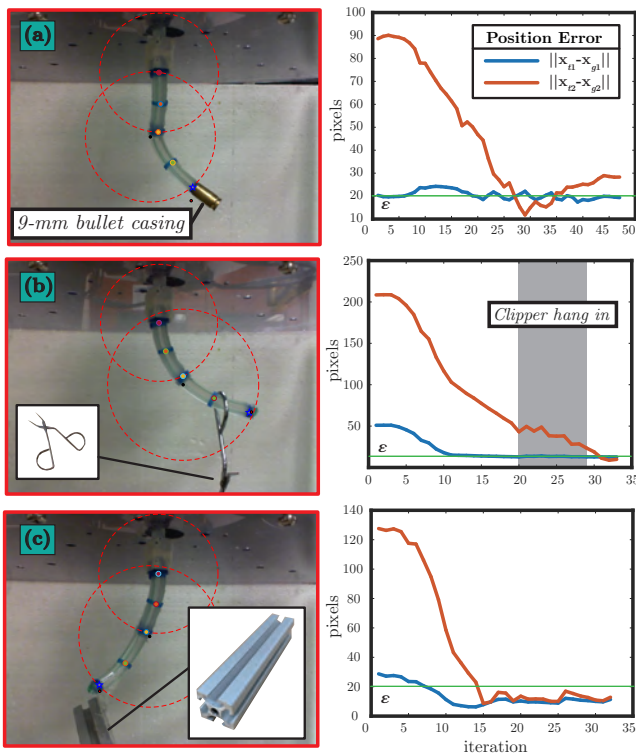
Fig. 10. Adaptive re-configuration with different payload. (a) Hitching a 9 mm bullet casing at the distal tip. The mass of the object is 3.8g, which is over 45% of the manipulator's weight; (b) suddenly hanging in a clipper manually while the manipulator is moving toward its goals. The mass of the object is 11.7g, which is over 140% of the manipulator's weight; (c) A aluminum bar with a weight of 47.6g is stuck on the distal segment using scotch tape. The object mass is 5.8 times over the manipulator itself.

the original place. The error plot shows that the proximal is able to steady maintain its gesture while manipulating the distal segment which is loaded with 45% of the manipulator's weight. Another case is shown in Fig. 10(b), where an object that is 140% the weight of the manipulator itself is suddenly hung on the distal segment. The gray area of the error chart demonstrates how the sudden intrusion can affect the distal end-effect position. But the manipulator can still be stabilized and got its job done. Fig. 10(c) shows the result of configuring the manipulator while it bears a weight of 47.6g, which is 5.8 times the mass of the manipulator.

V. CONCLUSIONS

In conclusion, this paper presents a vision-based method to adaptively control a two-segment cable-driven soft continuum robot manipulator in bi-direction. The controller is designed on the basis of IBVS method. Two segments can be steadily controlled by iteratively computing the reference segmental end-effectors' position. The soft manipulator can be shaped into multiple gestures as one can defined in image plane. The prototyping method of the proposed soft manipulator is given. The employment of PDMS in soft robot makes the manipulator soft, flexible, and elastic. Since PDMS is an inexpensive material, which is also nontoxic to human, it has the potential to be used in surgical continuum robotic tools.

The experiment indicates a satisfactory result in terms of shape control and payload capacity. The robot is able to carry a weight which is nearly 6 times of the manipulator's weight itself. Since the actuation mechanism of the manipulator (6 inputs) is designed for 3D maneuvering, future works may be addressed on fix-end (position and orientation) control and 3D visual servoing control using stereo-vision.

REFERENCES

[1] G. S. Chirikjian, "A continuum approach to hyper-redundant manipulator dynamics," in *Proceedings of 1993 IEEE/RSJ International Conference on Intelligent Robots and Systems (IROS '93)*, vol. 2, July 1993, pp. 1059–1066.

[2] R. J. Webster III and B. A. Jones, "Design and kinematic modeling of constant curvature continuum robots: A review," *The International Journal of Robotics Research*, vol. 29, no. 13, pp. 1661–1683, 2010.

[3] S. Kim, C. Laschi, and B. Trimmer, "Soft robotics: a bioinspired evolution in robotics," *Trends in biotechnology*, vol. 31, no. 5, pp. 287–294, 2013.

[4] J. Burgner-Kahrs, D. C. Rucker, and H. Choset, "Continuum robots for medical applications: A survey," *IEEE Transactions on Robotics*, vol. 31, no. 6, pp. 1261–1280, 2015.

[5] H. Banerjee, Z. T. H. Tse, and H. Ren, "Soft robotics with compliance and adaptation for biomedical applications and forthcoming challenges," *International Journal of Robotics and Automation*, vol. 33, no. 1, 2018.

[6] C. Della Santina and D. Rus, "Control oriented modeling of soft robots: the polynomial curvature case," *IEEE Robotics and Automation Letters*, vol. 5, no. 2, pp. 290–298, 2019.

[7] H. Wang, M. Totaro, and L. Beccai, "Toward perceptive soft robots: Progress and challenges," *Advanced Science*, vol. 5, no. 9, p. 1800541, 2018.

[8] H. Zhao, K. O'Brien, S. Li, and R. F. Shepherd, "Optoelectronically innervated soft prosthetic hand via stretchable optical waveguides," *Science Robotics*, vol. 1, no. 1, p. eaai7529, 2016.

[9] Y.-L. Park, K. Chau, R. J. Black, and M. R. Cutkosky, "Force sensing robot fingers using embedded fiber bragg grating sensors and shape deposition manufacturing," in *Proceedings 2007 IEEE International Conference on Robotics and Automation*. IEEE, 2007, pp. 1510–1516.

[10] Y.-L. Park, B.-R. Chen, and R. J. Wood, "Design and fabrication of soft artificial skin using embedded microchannels and liquid conductors," *IEEE Sensors Journal*, vol. 12, no. 8, pp. 2711–2718, 2012.

[11] J. C. Case, M. C. Yuen, J. Jacobs, and R. Kramer-Bottiglio, "Robotic skins that learn to control passive structures," *IEEE Robotics and Automation Letters*, vol. 4, no. 3, pp. 2485–2492, 2019.

[12] H. Wang, B. Yang, Y. Liu, W. Chen, X. Liang, and R. Pfeifer, "Visual servoing of soft robot manipulator in constrained environments with an adaptive controller," *IEEE/ASME Transactions on Mechatronics*, vol. 22, no. 1, pp. 41–50, Feb 2017.

[13] G. Fang, X. Wang, K. Wang, K.-H. Lee, J. D. Ho, H.-C. Fu, D. K. C. Fu, and K.-W. Kwok, "Vision-based online learning kinematic control for soft robots using local gaussian process regression," *IEEE Robotics and Automation Letters*, vol. 4, no. 2, pp. 1194–1201, 2019.

[14] A. V. Kudryavtsev, M. T. Chikhaoui, A. Liadov, P. Rougeot, F. Spindler, K. Rabenorosoa, J. Burgner-Kahrs, B. Tamadazte, and N. Andreff, "Eye-in-hand visual servoing of concentric tube robots," *IEEE Robotics and Automation Letters*, vol. 3, no. 3, pp. 2315–2321, 2018.

[15] R. Wang, S. Wang, E. Xiao, K. Jindal, W. Yuan, and C. Feng, "Real-time soft robot 3d proprioception via deep vision-based sensing," *ArXiv*, vol. abs/1904.03820, 2019.

[16] D. Bruder, B. Gillespie, C. D. Remy, and R. Vasudevan, "Modeling and control of soft robots using the koopman operator and model predictive control," *arXiv preprint arXiv:1902.02827*, 2019.

[17] F. Renda, M. Giorelli, M. Calisti, M. Cianchetti, and C. Laschi, "Dynamic model of a multibending soft robot arm driven by cables," *IEEE Transactions on Robotics*, vol. 30, no. 5, pp. 1109–1122, 2014.

[18] É. Marchand, F. Spindler, and F. Chaumette, "Visp for visual servoing: a generic software platform with a wide class of robot control skills," *IEEE Robotics & Automation Magazine*, vol. 12, no. 4, pp. 40–52, 2005.